

Infrared Spectrum of CH₃CN–BF₃ in Solid Argon

Nathan P. Wells and James A. Phillips*

Department of Chemistry, University of Wisconsin–Eau Claire, 105 Garfield Ave.,
Eau Claire, Wisconsin 54702

Received: August 23, 2001; In Final Form: December 3, 2001

We have observed and assigned several vibrational bands of 6 isotopomers of the CH₃CN–BF₃ complex in argon matrices. These include, for the parent isotopomer (CH₃CN–¹¹BF₃), the asymmetric BF₃ stretch (ν_{13}) at 1248 cm⁻¹, the BF₃ symmetric deformation or “umbrella” band (ν_7) at 601 cm⁻¹, and the C–N stretch (ν_2) at 2365 cm⁻¹. All of these bands require both CH₃CN and BF₃, grow slightly upon annealing to 20 K, display consistent relative intensities across all sample conditions studied, and have isotopic shifts that agree well with ab initio predictions. We observe the ν_2 band of CD₃CN–BF₃ at 2363 cm⁻¹, 17 cm⁻¹ to the red of a prior observation, though still only 7 cm⁻¹ from the frequency observed for crystalline CD₃CN–BF₃. The ν_{13} and ν_7 bands, however, are shifted by about 50 and 200 cm⁻¹ from the corresponding bands in the crystal, respectively. In turn, this indicates that the structure and bonding of matrix-isolated CH₃CN–BF₃ must differ significantly from the crystalline form of the complex.

Introduction

The 1:1 adduct formed from acetonitrile and boron trifluoride belongs to a novel class of donor acceptor complexes with structural properties that challenge the long held distinction between bonded and nonbonded interactions. Leopold and co-workers have characterized the structure and bonding of many such complexes^{1–3} and have called them *partially bonded molecules*¹ in reference to donor–acceptor interactions that are apparently intermediate between van der Waals forces and bona fide chemical bonds. As far as nitrogen donor–boron trifluoride systems are concerned, the structures of the gas phase complexes studied to date exhibit an enormously wide range of B–N distances that vary systematically with donor strength and span the entire range between those characteristic of weak interactions and strong dative bonds.¹ Specifically, amine complexes (e.g., H₃N–BF₃)⁴ display short B–N distances, about 1.6 Å, and a near tetrahedral geometry about the boron. At the other extreme, N₂–BF₃,⁵ a true “van der Waals molecule”, has a 2.88 Å B–N distance, and the BF₃ moiety retains its normal, planar geometry in the complex. Remarkably, CH₃CN–BF₃ exhibits a B–N distance of 2.011 Å and an N–B–F angle of 95.6° in the gas phase,⁶ clearly intermediate relative to the purely “van der Waals” and “chemical” cases cited above.

Computational studies of partially bonded molecules^{3,7–9} have been largely consistent with experiments and have demonstrated a large dynamic range in complex binding energies that parallels the structures. Surprisingly, however, computations have failed to reproduce the experimental structure of CH₃CN–BF₃.^{8,9} The most recent study predicts a B–N distance of 1.80 Å, an N–B–F angle of 101.2°, and a binding energy of 7.2 kcal/mol.⁸ Previously, B–N distances ranging from 2.17 to 2.28 Å, N–B–F angles ranging from 93 to 98°, and binding energies ranging from 4.0 to 7.2 kcal/mol were reported in three different studies.⁹ Together, these studies and the recent results actually bracket the experimental structural parameters.⁶ Thus, while

the intermolecular bond in CH₃CN–BF₃ is perhaps only slightly stronger than a good hydrogen bond, the binding energy could be one-third of that for H₃N–BF₃.^{10,11} Thus, computations also suggest fractional bonding, despite the peculiar discrepancy between the experimental and theoretical structures.

Yet another remarkable feature of partially bonded molecules is their inherent sensitivity to chemical environment. This is most clearly illustrated by comparisons of gas and crystal phase structures, which show that crystallization causes a dramatic contraction of the donor–acceptor bond and, in turn, furthers the geometrical distortion of the acceptor. For CH₃CN–BF₃, the crystal structure has a B–N distance of 1.630 Å and an N–B–F angle of 105.3°.¹² Thus, upon crystallization, the donor–acceptor bond contracts by about 0.4 Å, and the N–B–F angle opens by about 10°. There is chemical evidence that a solvent environment has an analogous effect on organofluoride–BF₃ complexes,¹ and investigations of small clusters¹³ and microsolvated species¹⁴ indicate that the dative bonds in these complexes contract significantly during the earliest stages of aggregation.

We are interested in the infrared spectra of partially bonded molecules, with an eye toward complex-induced shifts in the monomer bands, which should reflect the response of the constituent molecule's force fields to the incipient bond. Because the crystalline complexes usually have fully formed bonds,¹ and most lack any appreciable vapor pressure or are dissociated in the gas phase, we have chosen to study the complexes in argon matrices, a presumably nonperturbing environment. Regardless, differences between matrix and crystal-phase IR spectra should provide additional insight into the nature and extent of medium-induced differences in structure and bonding. With this intent, Beattie and Jones,¹⁵ investigated the C–N stretching frequency of CD₃CN–BF₃ in solid argon and observed the band at 2380 cm⁻¹, only slightly shifted relative to the crystalline value of 2373 cm⁻¹.¹⁶ Thus, they concluded that the structure of matrix-isolated CD₃CN–BF₃ very closely resembled that of the crystalline complex. Though this was perhaps surprising, recent matrix-IR investigations have demonstrated that argon matrices

* To whom correspondence should be addressed. Phone: 715-836-5399. Fax: 715-836-4979. E-mail: phillija@uwec.edu.

can substantially enhance hydrogen bond strength in amine–hydrogen halide complexes, as evidenced by host gas dependences of the complexes' vibrational frequencies, especially for H–X stretching bands.¹⁷

In this manuscript, we describe our recent investigation of the IR spectrum of CH₃CN–BF₃ in solid argon. We have dramatically extended the previous work¹⁵ and have assigned several new vibrational bands among 6 distinct isotopic forms of the complex. This includes two specific bands that correspond to motions occurring largely within the BF₃ moiety. Furthermore, we have observed the C–N stretching band at a significantly lower frequency than Beattie and Jones,¹⁵ and have confirmed this assignment with ¹⁵N isotopic substitution. In short, our observations are at odds with the notion that the structure and bonding of the matrix-isolated complex closely resembles that of its crystalline counterpart. There is, however, some ambiguity with regard to what complex-induced shifts in the C–N stretch and the BF₃ asymmetric stretch and umbrella modes are suggesting about the structure and bonding of the matrix-isolated complex. This is particularly significant, because shifts in ligand vibrational frequencies typically parallel binding strength,¹⁸ and the C–N stretch has been used to probe of the interaction of CH₃CN with BF₃,^{8,15,16,19–22} and other molecular Lewis acids,^{19–28} as well as metal ions and complexes in solution.^{18,21,29,30}

Experimental Section

All experiments were conducted using a newly assembled matrix isolation apparatus, based on a Cryomech ST15 optical cryostat cooled by a two stage, closed-cycle He refrigerator. The apparatus has a rotating optical cube fitted with KBr windows. The system is evacuated with a turbomolecular pump (Balzers/Pfeiffer TCP 121), which with the cold head, is mounted on a cart that allows the cryogenic sample to be transferred between experiments. The optical cube is fitted with a flange designed to enable simultaneous deposition from two separate lines containing mixtures of mutually reactive gases, which are mixed concentrically in a variable-length channel as they enter the cryostat chamber, about 1 in. from the cold window.

In the current study, we examined a wide range of sample conditions. Guest–host ratios of the individual gas mixtures usually ranged from 1/400 to 1/1000 (CH₃CN or BF₃/Ar), and because the flow rates through each line were nearly equal, the composition ratios in the matrix ranged from 1/1/800 to 1/1/2000 (CH₃CN/BF₃/Ar). For most experiments, we ran 3–5 successive 45–90 min depositions, flowing at 8–15 mmol/hr, with the cold window held between 8.5 and 15 K. Spectra were collected between each deposition. Most samples were subsequently annealed to about 20 K. We also performed a few experiments with higher reactant concentrations, up to about 1%, and annealed a few samples more aggressively, to about 30 K, in an attempt to produce aggregated or bulk-phase complexes (see below).

All spectra were recorded with a Nicolet Avatar 360 FTIR, at 1 cm⁻¹ resolution. BF₃ was obtained from Matheson and used without further purification. CH₃CN was obtained from Aldrich and distilled from CaH₂. CD₃CN and CH₃C¹⁵N were obtained from Cambridge Isotope Labs. In these instances, a small amount of CaH₂ was added directly to the sample tube containing the liquid, just before it was attached to the vacuum line used for preparing the gas mixtures. All CH₃CN samples were degassed via several freeze–pump–thaw cycles immediately prior to use.

TABLE 1: Observed IR Frequencies^a of CH₃CN–BF₃

isotopomer	ν_{13}^b	ν_7	ν_2
CH ₃ CN– ¹¹ BF ₃	1248	601	2365
CH ₃ CN– ¹⁰ BF ₃	1293	617	2365
CD ₃ CN– ¹¹ BF ₃	1250	601	2363
CD ₃ CN– ¹⁰ BF ₃	1291	618	2363
CH ₃ C ¹⁵ N– ¹¹ BF ₃	1249	601	2339
CH ₃ C ¹⁵ N– ¹⁰ BF ₃	1292	619	2339

^a All frequencies are reported in units of cm⁻¹ and are reproducible to within 1 cm⁻¹, consistent with the instrumental resolution. ^b Each observed ν_{13} band exhibits a secondary splitting which is observed about 9 cm⁻¹ higher in frequency. See text for discussion.

Results

In our initial attempts to identify CH₃CN–BF₃ in our matrices, we focused our attention on the C–N stretching region (2200–2400 cm⁻¹), because of the prior investigation of CD₃CN–BF₃.¹⁵ However, the only absorption feature we observed near the previously reported C–N stretching band at 2380 cm⁻¹ was readily observable in the absence of acetonitrile. At the time, we were only somewhat surprised by our inability to observe the previously reported absorption band, because it had been assigned to the fully deuterated isotopomer, and we were depositing CH₃CN in the matrix. CD₃CN was used previously to avoid the Fermi resonance in CH₃CN^{26,27} (see below), which does complicate the notion of a complexation shift. So, while theoretical calculations had predicted a minimal deuterium isotope shift for the C–N band, this issue was not clear initially, because we did not know whether the Fermi resonance would persist in the complex. This, together with the abundance of absorption features in this region, as well as interference from background CO₂, caused us to shift our attention to other regions of the spectrum. Ultimately, we obtained definitive assignments for three bands in each of 6 isotopic species and a tentative assignment for another. All require both CH₃CN and BF₃, grow slightly upon annealing to 20 K, and have consistent relative intensities (within 10%) across a wide range of sample conditions. Frequencies and assignments for these bands are listed in Table 1, and representative spectra are shown in Figures 1–3. Below, we describe our observations and additional rationale for these assignments with reference to the three spectral regions displayed in the figures. We note that the mode-numbering scheme used for the complex is that from Cho and Chong,⁸ which does differ somewhat from that used by Swanson and Shriver for the crystalline complex.¹⁶

BF₃ Asymmetric Stretching Region: 1200–1500 cm⁻¹. Figure 1 shows representative spectra of CH₃CN (i) and BF₃ (ii) in Ar, as well as both BF₃ and CH₃CN in Ar (iii), in the region of the asymmetric B–F stretching bands. The dominant spectral features in this region are the very strong asymmetric stretching bands (ν_3) of uncomplexed ¹⁰BF₃ and ¹¹BF₃ at 1492 and 1441 cm⁻¹, respectively.³¹ Most of the smaller peaks near the ν_3 band of BF₃, between 1350 and 1525 cm⁻¹, are absent in the CH₃CN/Ar spectra and have been assigned previously to BF₃ aggregates.³¹ In iii, about 200 cm⁻¹ below the ν_3 bands of BF₃ is a pair of peaks at 1293 and 1248 cm⁻¹ that clearly require both CH₃CN and BF₃. Both are split, and their secondary components appear at 1306 and 1257 cm⁻¹, respectively. They exhibit a 4:1 intensity ratio, which remains constant across all sample conditions, and is consistent with the relative natural abundance of ¹¹B and ¹⁰B. The measured splitting (45 cm⁻¹) differs only slightly from the observed ¹¹B–¹⁰B isotope shift (51 cm⁻¹) for the ν_3 band of uncomplexed BF₃ and is very consistent with the ab initio prediction (48 cm⁻¹)⁸ of the shift for the BF₃ asymmetric stretch in the complex (ν_{13}). Therefore,

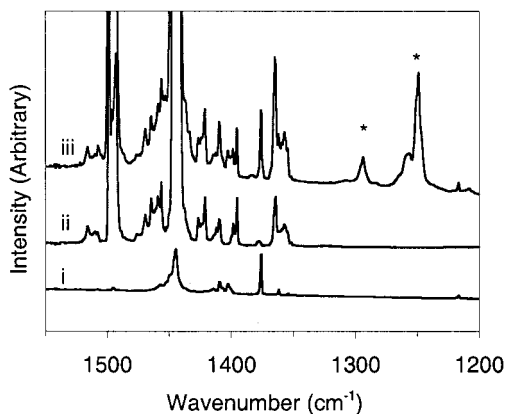


Figure 1. Representative spectra of the BF_3 asymmetric stretching region for matrices containing (i) CH_3CN in argon (1/400), (ii) BF_3 in argon (1/400), and (iii) CH_3CN and BF_3 in argon (1/1/800). Peaks assigned to the $\text{CH}_3\text{CN}-\text{BF}_3$ adduct are indicated with asterisks.

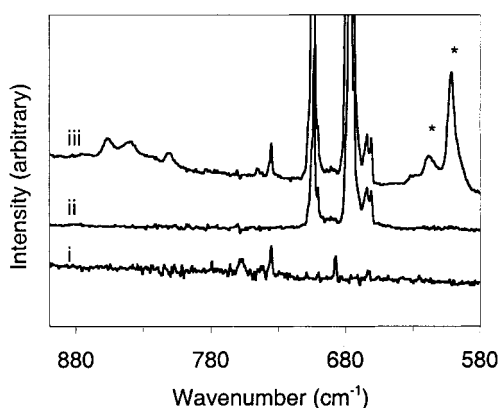


Figure 2. Representative spectra of the 580–900 cm^{-1} region for matrices containing (i) CH_3CN in argon (1/400), (ii) BF_3 in argon (1/400), and (iii) CH_3CN and BF_3 in argon (1/1/800). Peaks assigned to the $\text{CH}_3\text{CN}-\text{BF}_3$ adduct are indicated with asterisks.

we assign the peaks at 1248 and 1293 cm^{-1} to ν_{13} of the ^{11}B and ^{10}B isotopomers of $\text{CH}_3\text{CN}-\text{BF}_3$, respectively. Isotopic substitution experiments, involving nuclei on the CH_3CN unit (^{15}N and D), for which the isotope shifts are predicted by the calculations to be negligible,⁸ lend additional confidence to these assignments. The frequencies of the ν_{13} bands in the fully deuterated and ^{15}N isotopomers listed in Table 1 differ by only 1 cm^{-1} from the CH_3CN complexes. We note that the ν_{13} frequencies we observe are shifted by about 50 cm^{-1} from those of the crystalline complexes, for which a pair of peaks are observed at 1188 and 1208 cm^{-1} for $\text{CH}_3\text{CN}-^{11}\text{BF}_3$.¹⁶ It is also worthy on mentioning that they differ by only about 10 cm^{-1} from those predicted for the gas-phase complex (1260 cm^{-1} for $\text{CH}_3\text{CN}-^{11}\text{BF}_3$).⁸

Region of the ν_6 and ν_7 Modes: 580–900 cm^{-1} . Figure 2 shows representative spectra of the 580–900 cm^{-1} region for CH_3CN in Ar (i), BF_3 in Ar (ii), as well as CH_3CN and BF_3 in Ar (iii). The BF_3/Ar spectrum is dominated by several features between 650 and 710 cm^{-1} that have been assigned previously to the ν_2 symmetric deformation bands of BF_3 and BF_3 clusters.³¹ The $\text{CH}_3\text{CN}/\text{Ar}$ spectrum (ii) shows only a few weak features, including a CH_3CN combination band at approximately 735 cm^{-1} .³² In the $\text{CH}_3\text{CN}/\text{BF}_3/\text{Ar}$ spectrum (iii), about 80 cm^{-1} below the BF_3 monomer bands, are two features at 601 and 617 cm^{-1} that are absent in i and ii and have consistent 4:1 relative intensity ratio, reminiscent of a $^{10}\text{B}-^{11}\text{B}$ isotopic pair. Furthermore, their intensities relative to the ν_{13} bands (assigned

above) are consistent across a wide range of conditions. The observed isotope splitting for the BF_3 deformation band (ν_2) in the uncomplexed molecule is 12 cm^{-1} , and that predicted for the analogous ν_7 band in $\text{CH}_3\text{CN}-\text{BF}_3$ is 16 cm^{-1} ,⁸ precisely what we observe. The D_3 and ^{15}N isotope shifts are predicted to be 1 cm^{-1} or less,⁸ and we observe none among the ^{11}B bands and shifts of only 1 or 2 cm^{-1} for the ^{10}B bands. Therefore, we assign the peaks at 601 and 617 cm^{-1} to the ν_7 bands of the ^{11}B and ^{10}B isotopomers of $\text{CH}_3\text{CN}-\text{BF}_3$, respectively. Those for the ^{15}N and D_3 isotopomers are as listed in Table 1. It is again worth noting that our observed frequencies for this band differ by over 200 cm^{-1} from those of the crystal (e.g., 359 cm^{-1} for $\text{CH}_3\text{CN}-^{11}\text{BF}_3$)¹⁶ but agree fairly well with the ab initio predictions (e.g., 574 cm^{-1} for $\text{CH}_3\text{CN}-^{11}\text{BF}_3$).⁸

Around 850 cm^{-1} , three additional features are apparent in the $\text{CH}_3\text{CN}/\text{BF}_3/\text{Ar}$ spectrum shown in Figure 2 that do not appear in i and ii. This is the region of the BF_3 symmetric stretching band, designated as ν_6 in the complex, and ν_1 in free BF_3 . This band is forbidden in uncomplexed BF_3 but is predicted to be as intense as ν_7 in the complex,⁸ because of the pyramidal distortion of the BF_3 unit. Our best candidate for this band is the peak at 856 cm^{-1} , but we offer this only as a tentative assignment. Its intensity ratios relative to the other assigned bands are much less reproducible, and the isotope shifts we observe are less consistent with the ab initio predictions.⁸

C–N Stretching Region: 2200–2400 cm^{-1} . The region of the C–N stretching band, displayed in Figure 3 parts A and B, is quite complicated by the presence of many absorption features, as well as interference from background CO_2 from 2310 to 2370 cm^{-1} , because we disrupt the instrument purge when we collect spectra with our cryostat. Figure 3A shows, once again, spectra of CH_3CN in Ar (i), BF_3 in Ar (ii), and both CH_3CN and BF_3 in Ar (iii). The features apparent in all three spectra at 2339 and 2345 cm^{-1} are due to a CO_2 impurity in the matrix.³³ The prominent features in the $\text{CH}_3\text{CN}/\text{Ar}$ spectra (i) are the Fermi resonance doublet (ν_2 and $\nu_3 + \nu_4$)^{26,27} of CH_3CN at 2293 and 2258 cm^{-1} , and the latter exhibits a secondary splitting at 2256 cm^{-1} . The features in the BF_3/Ar spectrum (ii), aside from CO_2 , are combination bands ($\nu_1 + \nu_3$) of uncomplexed BF_3 , and presumably, the weak features are due to BF_3 clusters.³¹ The lone feature in the $\text{CH}_3\text{CN}/\text{BF}_3/\text{Ar}$ spectrum that is absent in both i and ii appears at 2365 cm^{-1} and has consistent relative intensity ratios with the previously assigned ν_7 and ν_{13} peaks discussed above. As such, we assign it to the C–N stretching mode (ν_2) of $\text{CH}_3\text{CN}-\text{BF}_3$. The $^{10}\text{B}-^{11}\text{B}$ isotope shift is predicted to be negligible for this band; thus, our observation of a single peak lends additional confidence to this assignment and also demonstrates that complexation with BF_3 disrupts the Fermi resonance in the CH_3CN moiety. We note that the Fermi resonance does persist upon complexation with HF ²⁷ as well as with HfCl_4 and ZrCl_4 .²⁶

The fact that our observation of the ν_2 band was rather inconsistent with the previously reported value of 2380 cm^{-1} motivated us to pursue spectra of the D and ^{15}N labeled complexes to confirm our assignment. Spectra of CH_3CN (i), CD_3CN (ii), and $\text{CH}_3\text{C}^{15}\text{N}$ (iii) with BF_3 in Ar are shown in Figure 3B. One notable difference among the spectra is in the C–N bands (ν_2) of the uncomplexed CH_3CN species. In CD_3CN , the Fermi resonance is clearly absent and only a single peak is observed at 2267 cm^{-1} . For $\text{CH}_3\text{C}^{15}\text{N}$, two peaks are observed, as the Fermi resonance persists in the ^{15}N species.²⁷ As for the ν_2 band in the complex, the feature at 2363 cm^{-1} in the $\text{CD}_3\text{CN}/\text{BF}_3/\text{Ar}$ spectrum (ii) requires both CD_3CN and BF_3 , has consistent intensity ratios with the other assigned bands,

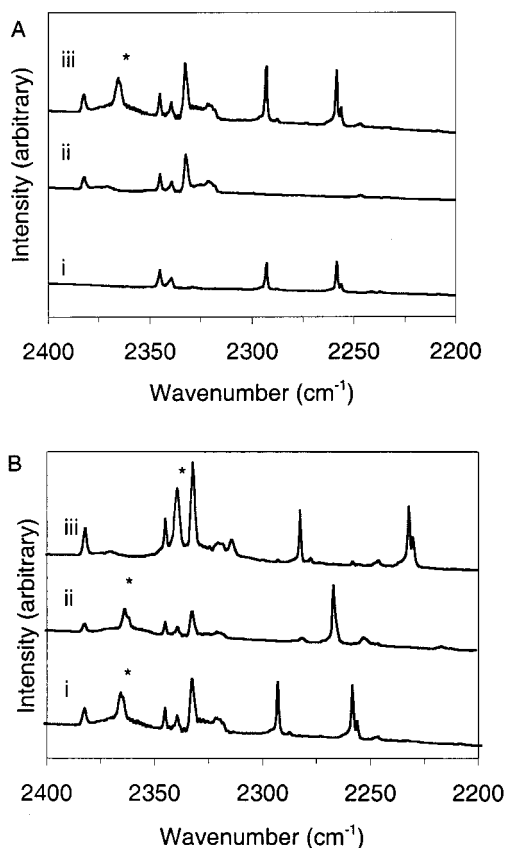


Figure 3. A. Representative spectra of the C–N stretching region for matrices containing (i) CH₃CN in argon (1/400), (ii) BF₃ in argon (1/400), and (iii) CH₃CN and BF₃ in argon (1/1/800). The peaks assigned to the CH₃CN–BF₃ adduct are indicated with asterisks. B. Representative spectra of the C–N stretching region showing the effects of D and ¹⁵N isotopic substitution. Trace i is the spectrum obtained with CH₃CN and BF₃ in argon (1/1/800), ii was obtained with CD₃CN and BF₃ in argon (1/1/800), and iii was obtained with CH₃C¹⁵N and BF₃ in argon (1/1/800). In each, the asterisk denotes the C–N stretching band.

and lies very near the ν_2 band of CH₃CN–BF₃. No deuterium isotope shift was predicted for the C–N stretching band in the complex,⁸ but given that the observed shift is small (2 cm⁻¹) and this region has been somewhat obscured by interference from CO₂, we deem the agreement to be satisfactory. Thus, we assigned this feature to ν_2 of CD₃CN–BF₃ and note that the only absorption feature we observe near at 2380 cm⁻¹ in the deuterium isotopic substitution experiments is clearly visible in the Ar/BF₃ spectrum (i) in Figure 3A.

When we first examined the CH₃C¹⁵N/BF₃/Ar spectra, we were initially struck by the absence of a new band attributable to ν_2 of CH₃C¹⁵N–BF₃. However, upon closer inspection, we noticed that the intensity of the 2339 cm⁻¹ peak that is due to CO₂³³ had grown dramatically relative to its counterpart and realized that the band we sought was coincident with it. Thus, the relative intensity ratios of this band to the other assignments are slightly less consistent than for the other assignments. In any event, the observed ¹⁴N–¹⁵N isotope shift of 26 cm⁻¹ agrees well with the predicted value of 30 cm⁻¹, and we therefore assign this band to ν_2 of CH₃C¹⁵N–BF₃. An examination of Figure 3B clearly shows that aside from the peaks assigned to ν_2 in the complex, or the C–N stretches in the free nitriles, the spectra are virtually identical. We view this as very convincing evidence that our assignments are correct, despite the discrepancy with previously reported ν_2 frequency for the CD₃CN–BF₃.¹⁵

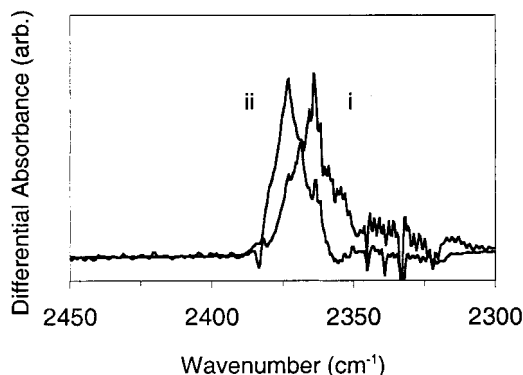


Figure 4. Subtraction spectra showing the effects of annealing to 20 and 30 K. Trace i was obtained by subtracting the spectrum of a freshly deposited CH₃CN/BF₃/Ar matrix (1/1/800), from that obtained after annealing the sample to 20 K for 20 min. Trace ii was obtained by subtracting the unannealed data from a spectrum recorder after 20 min of annealing to 30 K. The peak in i coincides with our assignment of ν_2 in the “isolated” complex, and that in ii coincides with the C–N stretching frequency of crystalline CH₃CN–BF₃. See text for discussion.

Ultimately, the discrepancy led us to speculate that the 2380 cm⁻¹ band observed previously was due to larger aggregates of the complex (e.g., (CH₃CN–BF₃)_n), because the conditions in that investigation were in fact much richer in BF₃.¹⁵ To pursue this notion, we examined some matrices with richer conditions and conducted some additional annealing experiments. With richer matrices, up to 1% BF₃ and/or CH₃CN, the only new bands we observed were essentially coincident with those of the crystalline compound.¹⁶ Annealing relatively dilute matrices more aggressively yielded the spectra shown in Figure 4. Trace i, with the peak at the right (2363 cm⁻¹), was obtained by subtracting the spectrum of a freshly deposited CD₃CN/BF₃/Ar matrix (about 1/1/800) from that of the same matrix after 20 min of annealing at 20 K. The peak in i is coincident with our assignment of ν_2 and shows definitively that the band we assigned to the C–N stretch in the 1:1 complex does grow upon annealing. Spectrum ii was obtained by subtracting the unannealed data from the spectrum recorded immediately after annealing to 30 K for 20 min. The peak in ii lies at 2373 cm⁻¹, coincident with the observed C–N stretch in the crystal.¹⁶ This demonstrates that we can produce “crystalline-like” CH₃CN–BF₃ in our matrices, but we fail to see any absorption feature at 2380 cm⁻¹. The exception is, again, the band that is discernible in the Ar/BF₃ spectrum in Figure 3A, which also lacks the proper intensity ratios and annealing behavior. Therefore, we can offer no explanation for the discrepancy with the previous assignment of ν_2 .¹⁵

Discussion

The observation of two new vibrational bands that involve motion of the B–F bonds, as well as our new assignment for the C–N stretch, warrants a reevaluation of the conclusion stated previously, that the structure and bonding of matrix-isolated CH₃CN–BF₃ closely resembles that of the crystalline compound.¹⁵ Of course, our insight is only indirect and is based solely on a comparison of our measurements with the vibrational frequencies of the crystal.¹⁶ Unfortunately, the only frequencies available for the gas-phase complex come from the recent computations,⁸ and although these agree fairly well with our measurements, they stem from a structure that differs markedly from experiment. As such, we cannot draw any conclusions at this point as to how the structure and bonding of matrix-isolated CH₃CN–BF₃ may compare to that of the gas-phase complex.

For the purpose of simplifying this discussion, all frequencies referred to henceforth are those of the parent isotopomer ($\text{CH}_3\text{CN}^{11}\text{BF}_3$) unless otherwise noted. In summary, we observe the BF_3 asymmetric stretching mode (ν_{13}) at 1248 cm^{-1} (with a weaker splitting at 1257 cm^{-1}), $40\text{--}50\text{ cm}^{-1}$ from the crystal bands (1188 and 1208 cm^{-1}) and only 12 cm^{-1} from the ab initio prediction (1260 cm^{-1}). Further, we observe the BF_3 “umbrella” band (ν_7) at 601 cm^{-1} , over 200 cm^{-1} from the crystal value of 359 cm^{-1} and just 27 cm^{-1} from the ab initio prediction. However, we observe the C–N stretching band at 2365 cm^{-1} , only slightly different from that of the crystal (2373 cm^{-1}) and about 60 cm^{-1} to the blue of the prediction (2302 cm^{-1}). Clearly, the BF_3 -localized modes indicate that the structure and bonding of the matrix-isolated complex differs from the crystalline species. The C–N stretch, on the other hand, suggests a complex that is similar to the crystalline form, even though we reassigned the band to a frequency that is 17 cm^{-1} to the red of the previously quoted value (for $\text{CD}_3\text{CN}^{15}$).

The apparent discrepancy between the vibrational band shifts of the donor and acceptor led us to the vast literature concerning the characteristic C–N blue shift in nitrile and cyano complexes, which has been the subject of numerous investigations over the past four decades.^{8,15,18–30,34} Apparently, this shift was once thought to result from coupling to the C–C stretching mode,^{8,20,34} but by most accounts,^{8,20–23,28,34} it stems from a genuine increase in the C–N force constant, consistent with the fact that the C–N bond distance contracts upon complexation with BF_3 .^{12,35} One recent study used an empirical model to demonstrate that an “accumulation of charge” in the C–N bonding region causes the bond to stiffen.²⁸ This is consistent with the previously stated notion that the σ_{CN} and π_{CN} bonding orbitals of CH_3CN are stabilized upon complexation.^{21–23,34} However, although the underlying cause of the C–N blue shift has been explained, there are indications that the magnitude of this shift is a rather unreliable indicator of C–N coordinate bond strength. For instance, Purcell has argued that cyanide frequency shifts can be very misleading and that it is critical to base structural interpretations on the force constants themselves.³⁴ Similarly, Beattie used a normal-mode analysis of $\text{CH}_3\text{CN}^{20}$ to demonstrate that the C–N stretching frequency is “remarkably insensitive” to coordinate bond strength. Although recent studies of CH_3CN –metal ion complexes^{29,30} indicate that the blue shift does parallel cation charge density, no similar trend is apparent upon an analogous examination of complexes with molecular Lewis acids. Even among complexes of the boron halides, for which the relative Lewis acidity is well established, the observed C–N frequencies are 2376 , 2380 , and 2350 cm^{-1} for the BF_3 , BCl_3 , and BBr_3 adducts, respectively.^{16,23} Clearly, these data follow no trend, but we note that the values cited are all from the solid phase, and it is likely that medium effects (i.e., gas–solid structure differences) are obscuring any would-be trend. Regardless, the C–N shifts observed for $\text{CH}_3\text{CN}^{15}$ in various media do not show a clear trend either. Presumably, the complex is least strongly bonded in the matrix, somewhat more strongly bonded in solution, and is in fact fully bonded in the solid phase.¹² In turn, one might expect the C–N stretching band to shift accordingly. However, in solution, the C–N stretch lies around 2355 cm^{-1} ^{19,21,36} which is to the red of both the crystal (2376 cm^{-1})¹⁶ and matrix (2365 cm^{-1}) values, and the frequency is largely independent of solvent.^{19,21,36} Clearly, these observations cast some doubt upon interpretations of the magnitude of the C–N blue shift in terms of complexation strength, and the discrepancy we observe between the shifts in the nitrile stretch and BF_3 -localized bands only adds to this.

Aside from the issues relating to the C–N stretch, there are other reasons that the BF_3 -localized modes could be viewed as a more reliable indicator of the extent of complexation. Given that the out-of-plane distortion of the BF_3 unit must disrupt π overlap and reduce the double bond character of the B–F bonds, it must also lower the B–F stretching (k_1) and out-of-plane bending (k_Δ) force constants. Furthermore, for a pyramidal XY_3 -type molecule (a distorted BF_3 unit), the valence-force expressions for the vibrational frequencies depend explicitly on the out-of-plane distortion angle,³⁷ which differs by 10° between the gas- and crystal-phase forms of $\text{CH}_3\text{CN}^{15}$.^{6,12} Moreover, a recent computational study of a few similar nitrile– BF_3 complexes,³⁸ which is in good agreement with experimental structural results for HCN^{39} and N_2^{5} – BF_3 ,⁵ found nearly linear correlations between complex-induced shifts in BF_3 -localized vibrational bands and complex binding energy. A cursory examination of these results also indicates that these frequency shifts also parallel structural properties, specifically B–N distance and N–B–F angle.

In light of this, it is tempting to simply dismiss the C–N stretching band we observe as an anomaly, and conclude that the structure and bonding of matrix-isolated $\text{CH}_3\text{CN}^{15}$ – BF_3 closely resembles that of the gas-phase complex. However, this notion would rest upon the cited computational results,⁸ which again, fail to reproduce the experimental structure.⁶ So at this point, we can only state that the structure and bonding of the matrix-isolated complex does differ significantly from its crystalline counterpart, and we emphasize that the basis for this conclusion is differences between the measured ν_{13} and ν_7 frequencies of the crystalline and matrix-isolated complexes. Furthermore, because all of the matrix-isolated bands are shifted toward the analogous free molecule bands, it appears that the matrix-isolated complex must have a “less fully developed” B–N dative bond than in the crystal (i.e., with longer B–N distance and a smaller N–B–F angle). Even the ν_2 band we observe is consistent with this notion, because the complex-induced C–N blue shift is less in the matrix than in the crystal.¹⁶ The recent theoretical examinations of BF_3 -localized frequencies³⁸ support this idea further, not only by demonstrating that the frequency shifts parallel the structural properties but also that the bands shift in a manner consistent with our interpretation of the matrix-crystal shifts for $\text{CH}_3\text{CN}^{15}$ – BF_3 . For example, for the BF_3 “umbrella” mode (ν_7 in the present case) was shown to red shift upon complexation and to be the most sensitive of the BF_3 -localized modes to complexation strength, with shifts ranging from 19.4 in N_2 – BF_3 to 66.6 cm^{-1} in HC_3N^{38} – BF_3 . We observe ν_7 about 75 cm^{-1} to the red of the umbrella band of uncomplexed BF_3 in the matrix, yet over 200 cm^{-1} to the blue of the ν_7 band of crystalline $\text{CH}_3\text{CN}^{15}$ – BF_3 . These comparisons also support the notion of a matrix-isolated complex with a B–N dative bond that is much less fully developed than in the crystal. Unfortunately, in the absence of a vapor-phase IR spectrum or, at the very least, a set of ab initio frequencies based on a structure that is consistent with experiment, it is impossible to assess how the structure and bonding of the matrix-isolated complex compares to that of the gas-phase adduct. In turn, it is difficult to gauge the exact nature and extent of the structural difference conveyed by the matrix–crystal frequency shifts.

Conclusions

We have observed several new vibrational bands of 6 isotopomers of $\text{CH}_3\text{CN}^{15}$ – BF_3 in argon matrices. These bands require the presence of both CH_3CN and BF_3 , have consistent

relative intensities across a wide range of sample conditions, grow slightly upon annealing to 20 K, and display isotope shifts that are remarkably consistent with recent ab initio predictions.⁸ Furthermore, we observe the C–N stretch of CD₃CN–BF₃ at 2363 cm⁻¹, about 17 cm⁻¹ lower in frequency than in a previous study,¹⁵ and have confirmed our assignment with ¹⁵N isotopic substitution. The observed frequencies we observe for the BF₃-localized vibrational modes (ν_{13} and ν_7) differ markedly from those observed for the crystalline compound,¹⁶ and these substantial matrix–crystal shifts indicate that the structure and bonding of the complex must differ significantly between the two environments. This is in great contrast to a previous report¹⁵ that indicated that the structures of matrix-isolated and crystalline CH₃CN–BF₃ were quite similar. However, because the gas phase IR spectrum of the complex has not been recorded and the only available ab initio frequencies are based on a structure that does not agree with experiment,⁶ additional work is needed to gauge the true effect of the matrix environment on the structure and bonding of the complex.

Acknowledgment for financial support of this work is made to the donors of the Petroleum Research Fund, administered by the American Chemical Society. This work was also supported by an award from Research Corporation. The University of Wisconsin–Eau Claire provided additional financial support and facilities. N.P.W. acknowledges a Jean Dreyfus Boissevain Undergraduate Scholarship for Excellence in Chemistry, sponsored by the Camille and Henry Dreyfus Foundation. We would also like to extend our appreciation to Dr. M. McEllistrem for his advice in designing the vacuum system for our cryostat.

References and Notes

- (1) Leopold, K. R.; Canagaratna, M.; Phillips, J. A. *Acc. Chem. Res.* **1997**, *30*, 57.
- (2) Burns, W. A.; Phillips, J. A.; Canagaratna, M.; Goodfriend, H.; Leopold, K. R. *J. Phys. Chem. A* **1999**, *103*, 7445.
- (3) Hunt, S. W.; Leopold, K. R. *J. Phys. Chem. A* **2001**, *105*, 5498.
- (4) Fujiang, D.; Fowler, P. W.; Legon, A. C. *J. Chem. Soc., Chem. Commun.* **1995**, 113.
- (5) Janda, K. C.; Bernstien, L. S.; Steed, J. M.; Novick, S. E.; Klemperer, W. *J. Am. Chem. Soc.* **1978**, *100*, 8074.
- (6) Dvorak, M. A.; Ford, R. S.; Suenram, R. D.; Lovas, F. J.; Leopold, K. R. *J. Am. Chem. Soc.* **1992**, *114*, 108.
- (7) Wong, M. W.; Wiberg, K. B.; Frisch, M. J. *J. Am. Chem. Soc.* **1992**, *114*, 523.
- (8) Cho, H.-G.; Cheong, B.-S. *J. Mol. Struct. (THEOCHEM)* **2000**, *496*, 185.
- (9) (a) Jurgens, R.; Almlöf, J. *Chem. Phys. Lett.* **1991**, *176*, 263. (b) Jiao, H. J.; Schleyer, P. v. R. *J. Am. Chem. Soc.* **1994**, *116*, 7429. (c) Jonas, V.; Frenking, G.; Reetz, M. T. *J. Am. Chem. Soc.* **1994**, *116*, 8741.
- (10) Nxumalo, L. M.; Andrzejak, M.; Ford, T. A. *Vib. Spectrosc.* **1996**, *12*, 221.
- (11) Jonas, V.; Frenking, G. *J. Chem. Soc. Chem. Commun.* **1994**, 1489.
- (12) Swanson, B.; Shiver, D. F.; Ibers, J. A. *Inorg. Chem.* **1969**, *8*, 2183.
- (13) Cabaleiro-Lago, E. M.; Rios, M. A. *Chem Phys. Lett.* **1998**, *294*, 272.
- (14) Fiacco, D. L.; Hunt, S. W.; Leopold, K. R. *J. Phys. Chem. A* **2000**, *104*, 8323.
- (15) Beattie, I. R.; Jones, P. J. *Angew. Chem. Int. Ed. Engl.* **1996**, *35*, 1527.
- (16) Swanson, B.; Shriver, D. F. *Inorg. Chem.* **1970**, *6*, 1406.
- (17) (a) Andrews, L.; Wang, X. F. *J. Phys. Chem. A* **2001**, *105*, 7541. (b) Andrews, L.; Wang, X. F.; Mielke, Z. *J. Phys. Chem. A* **2001**, *105*, 6054.
- (18) Nakamoto, K. *Infrared and Raman Spectra of Inorganic and Coordination Compounds. Part B: Application in Coordination, Organometallic, and Bioinorganic Chemistry*, 5th ed.; John Wiley and Sons: New York, 1997.
- (19) Coerver, H. J.; Curran, C. *J. Am. Chem. Soc.* **1958**, *80*, 3522.
- (20) Beattie, I. R.; Gilson, T. *J. Chem. Soc.* **1964**, 2292.
- (21) Purcell, K. F.; Drago, R. S. *J. Am. Chem. Soc.* **1966**, *88*, 919.
- (22) Hase, Y. *An. Acad. Bras. Cien.* **1987**, *59*, 299.
- (23) Shriver, D. F.; Swanson, B. *Inorg. Chem.* **1971**, *10*, 1354.
- (24) Kawano, Y.; Hase, Y.; Sala, O. *J. Mol. Struct.* **1976**, *30*, 45.
- (25) Watari, F. *J. Phys. Chem.* **1980**, *84*, 448.
- (26) Hase, Y.; Alves, O. L. *Spectrochim. Acta A* **1981**, *37*, 711.
- (27) Johnson, G. L.; Andrews, L. *J. Phys. Chem.* **1983**, *87*, 1852.
- (28) Vijay, A.; Sathyanarayana, D. N. *J. Phys. Chem.* **1996**, *100*, 75.
- (29) Fawcett, W. R.; Liu, G. *J. Phys. Chem.* **1992**, *96*, 4231.
- (30) Jamróz, D.; Wójcik, M.; Lindgren, J.; Stangret, J. *J. Phys. Chem. B* **1997**, *101*, 6758.
- (31) Nxumalo, L. M.; Ford, T. A. *Vib. Spectrosc.* **1994**, *6*, 333.
- (32) Freedman, T. B.; Nixon, E. R. *Spectrochim. Acta A* **1972**, *28*, 1375.
- (33) Knözinger, E.; Beichert, P. *J. Phys. Chem. A* **1995**, *99*, 4906.
- (34) Purcell, K. F. *J. Am. Chem. Soc.* **1967**, *89*, 6139.
- (35) Demaison, J.; Dubrulle, A.; Boucher, D.; Burie, J. *J. Mol. Spec.* **1979**, *16*, 1.
- (36) Burns, W. A. Unpublished results.
- (37) Herzberg, G. *Molecular Spectra and Molecular Structure, Volume II: Infrared and Raman Spectra of Polyatomic Molecules*; Krieger Publishing Co.: Malabar, FL, 1991.
- (38) Nxumalo, L. M.; Andrzejak, M.; Ford, T. A. *J. Mol. Struct.* **1999**, *509*, 287.
- (39) Reeve, S. W.; Burns, W. A.; Lovas, F. J.; Suenram, R. D.; Leopold, K. R. *J. Phys. Chem.* **1993**, *97*, 10630.
- (40) Hehre, W. J.; Random, L.; Schleyer, P. v. R.; Pople, J. A. *Ab initio Molecular Orbital Theory*; Wiley-Interscience: New York, 1986.